8-9-2013

Radiolytic mapping of solvent-contact surfaces in photosystem II of higher plants: Experimental identification of putative water channels within the photosystem

Laurie K. Frankel
Louisiana State University

Larry Sallans
University of Cincinnati

Henry Bellamy
Louisiana State University

Jost S. Goettert
Louisiana State University

Patrick A. Limbach
Louisiana State University

See next page for additional authors

Recommended Citation

Frankel, L., Sallans, L., Bellamy, H., Goettert, J., Limbach, P., & Bricker, T. (2013). Radiolytic mapping of solvent-contact surfaces in photosystem II of higher plants: Experimental identification of putative water channels within the photosystem. *Journal of Biological Chemistry, 288* (32), 23565-23572. https://doi.org/10.1074/jbc.M113.487033

THE JOURNAL OF BIOLOGICAL CHEMISTRY VOL. 288, NO. 32, pp. 23565–23572, August 9, 2013

Radiolytic Mapping of Solvent-Contact Surfaces in Photosystem II of Higher Plants

EXPERIMENTAL IDENTIFICATION OF PUTATIVE WATER CHANNELS WITHIN THE PHOTOSYSTEM[*][S]

Received for publication, May 21, 2013, and in revised form, June 27, 2013 Published, JBC Papers in Press, June 28, 2013, DOI 10.1074/jbc.M113.487033

Laurie K. Frankel[‡], **Larry Sallans**[§], **Henry Bellamy**[¶], **Jost S. Goettert**[¶], **Patrick A. Limbach**[§], **and Terry M. Bricker**[‡1]

From the [‡]*Department of Biological Sciences, Division of Biochemistry and Molecular Biology, Louisiana State University, Baton Rouge, Louisiana 70803, the* [§]*Rieveschl Laboratories for Mass Spectrometry, Department of Chemistry, University of Cincinnati, Cincinnati, Ohio 45221, and the* [¶]*J. Bennett Johnston, Sr. Center for Advanced Microstructures & Devices, Louisiana State University, Baton Rouge, Louisiana 70806*

Background: Substrate water must reach the buried Mn_4O_5Ca cluster in Photosystem II.
Results: $OH^{\bullet}$ produced by radiolysis modified buried amino acid residues. These were mapped onto the PS II crystal structure.
Conclusion: Two groups of oxidized residues were identified which form putative pathways to the Mn_4O_5Ca cluster.
Significance: Identification of water and oxygen channels is crucial for our understanding of Photosystem II function.

Photosystem II uses water as an enzymatic substrate. It has been hypothesized that this water is vectored to the active site for water oxidation via water channels that lead from the surface of the protein complex to the Mn_4O_5Ca metal cluster. The radiolysis of water by synchrotron radiation produces amino acid residue-modifying $OH^{\bullet}$ and is a powerful technique to identify regions of proteins that are in contact with water. In this study, we have used this technique to oxidatively modify buried amino acid residues in higher plant Photosystem II membranes. Fourier transform ion cyclotron resonance mass spectrometry was then used to identify these oxidized amino acid residues that were located in several core Photosystem II subunits (D1, D2, CP43, and CP47). While, as expected, the majority of the identified oxidized residues (≈75%) are located on the solvent-exposed surface of the complex, a number of buried residues on these proteins were also modified. These residues form groups which appear to lead from the surface of the complex to the Mn_4O_5Ca cluster. These residues may be in contact with putative water channels in the photosystem. These results are discussed within the context of a number of largely computational studies that have identified putative water channels in Photosystem II.

Photosystem II (PS II)[2] uses the energy harvested from light energy to oxidize water and reduce plastoquinone. Six intrinsic membrane proteins appear to be required for O_2 evolution. These are CP47, CP43, D1, D2, and the α and β subunits of cytochrome b_{559}. Deletion of any one of these subunits uniformly results in the loss of PS II function and assembly (1, 2). In higher plants, three extrinsic proteins, PsbO, PsbP, and PsbQ also are required for maximal rates of O_2 evolution under physiological inorganic cofactor concentrations (3). The PsbO protein appears to play a central role in the stabilization of the manganese cluster (4), is essential for efficient and stable O_2 evolution and is required, along with PsbP, for photoautotrophic growth and PS II assembly in higher plants propagated under normal growth conditions (5–8). Under low light growth conditions the PsbQ component also is required for photoautotrophy (8, 9). Over the past decade, increasingly higher resolution crystal structures of cyanobacterial PS II have significantly enhanced our understanding of the molecular organization of the constituent polypeptides of the photosystem and the active site for oxygen evolution, the Mn_4O_5Ca cluster (10–14). A high resolution, 1.9 Å crystal structure of cyanobacterial PS II has recently become available (15). Unfortunately, no crystal structures for higher plant PS II have been presented. While there are differences between the higher plant and the cyanobacterial photosystems, particularly with respect to the identity and organization of the extrinsic proteins (3), the amino acid sequences of the intrinsic components (D1, D2, CP43, and CP47) are very similar (>85% similarity (16)). Consequently, one would expect that the structural and functional organization of these proteins within PS II would be highly homologous between higher plants and cyanobacteria.

The use of the synchrotron radiolysis of water to produce $OH^{\bullet}$ capable of oxidatively modifying amino acid residues in contact with water is an emerging and useful technique in structural biology (17, 18). Recently, this method has been used to identify buried water molecules which function in a channel mediating the activation of a membrane protein, the G-protein-coupled receptor, rhodopsin (19). It has also been used to identify the surface residues of proteins that are exposed to the bulk aqueous solvent (20, 21).

* This work was supported by the Division of Chemical Sciences, Geosciences, and Biosciences, Office of Basic Energy Sciences of the U. S. Department of Energy through Grant DE-FG02-98ER20310 (to T. M. B. and L. K. F.). Additional support was provided by National Institutes of Health Grants RR019900 and GM58843 (to P. A. L.) and the State of Louisiana (to H. B. and J. S. G.).

[S] This article contains supplemental Fig. S1 and Tables S1–S4.

[1] To whom correspondence should be addressed: Department of Biological Sciences, Division of Biochemistry and Molecular Biology, Louisiana State University, Baton Rouge, LA 70803. Tel.: 225-578-1555; Fax: 225-578-2597; E-mail: btbric@lsu.edu.

[2] The abbreviations used are: PS II, Photosystem II; FT-ICR, Fourier transform ion cyclotron resonance; LiDS, lithium dodecyl sulfate; ROS, reactive oxygen species; S_n, oxidation states (n=1,2,3,4) of the Mn_4O_5Ca cluster.

Because the active site for water oxidation, the Mn_4CaO_5 cluster, is buried within the structure of the photosystem, substrate water must transit from the bulk solvent to the active site through water channels. Several largely computational studies have sought to identify these pathways. Murray and Barber (22) used the CAVER Program (23) to examine the 3.5 Å crystal structure of *Thermosynechococcus elongatus* (12). Gabdulkhakov *et al.* (24) used nobel gas and dimethyl sulfoxide co-crystallization studies in combination with CAVER to examine the 2.9 Å structure of *T. elongatus* (14), and Ho and Styring calculated solvent-accessible surfaces for the 3.0 Å *T. elongatus* structure of Loll *et al.* (13). Molecular dynamic simulations have also been used to probe for water channels within the photosystem (25, 26), the latter study being performed on the recent high resolution PS II structure (15).

We hypothesized that buried amino acid residues in contact with such putative water channels in the interior of PS II would be significantly more susceptible to oxidative amino acid modification during the synchrotron radiolysis of water than buried residues not exposed to water. Consequently, the identification of such oxidatively modified residues in the interior of PS II should serve to complement and extend the largely computational studies mentioned above.

EXPERIMENTAL PROCEDURES

PS II membranes were isolated from market spinach by the method of Berthold *et al.* as modified by Ghanotakis and Babcock (27, 28). After isolation, the PS II membranes were suspended at 2 mg chlorophyll/ml in 50 mM Mes-NaOH, pH 6.0, 300 mM sucrose, 15 mM NaCl buffer, and frozen at −80 °C until use. In these experiments, we have used the XLRM2 beamline at The J. Bennett Johnston, Sr. Center for Advanced Microstructures & Devices (CAMD) synchrotron. This beamline provides attenuated unfocused radiation which has been passed through a 100 μm beryllium and 25 μm aluminum filters to remove the low energy components. The maximum flux is near 4 keV. The photon flux absorbed by the sample was 1.58×10^6 photons/sec/μm^2. Consequently, at our longest exposure time of 16 s, the sample absorbed 2.5×10^7 photons/μm^2, which was equivalent to an absorbed dose of about 2.43×10^4 Gray. The end-station was modified to accommodate a Plexiglas chamber with machined channels (3 mm × 60 mm × 1 mm) to contain the PS II membrane samples. The samples were covered by 75 μm Kapton foil to retain the sample (≈180 μl). The individual channels were positioned in the beam by remote control and exposed for various lengths of time (0, 4, 8, 16 s) at room temperature. After exposure, the samples were immediately removed from the chamber and held on ice until being stored at −80 °C until further analysis.

The proteins in the samples were resolved on a 12.5–20% acrylamide gradient by LiDS-PAGE using a non-oxidizing gel system (29, 30). This was required, as standard PAGE is known to introduce numerous protein oxidation artifacts (29, 31). In the non-oxidizing system the gels are polymerized with riboflavin (in the presence of diphenyliodonium chloride + toluene sulfinate) followed by exposure to UV light. The upper reservoir contained thioglycolate. Preliminary experiments indicated that proteins resolved in this system exhibited much lower levels of artifactual protein oxidation than proteins resolved under standard LiDS-PAGE conditions (see Ref. 30, supplemental Fig. S1). After electrophoresis, the gels were stained with Coomassie Blue, destained, and protein bands containing CP47, CP43, D1, and D2 were excised. These were then processed for trypsin digestion using standard protocols. In some cases, the tryptic peptides were processed using a C18 ZipTip® prior to mass analysis.

Reversed-phase chromatography was performed as described previously (30) using a Finnigan Surveyor MS pump and a Finnigan Micro AS autosampler. A Waters X-Bridge C18 3.5 μm 2.1 × 100 mm column was used for the reversed phase separation of the tryptic peptides. It was operated at a flow rate of 200 μl/min. The mobile phases consisted of a 95:5 water:acetonitrile with 0.1% formic acid aqueous phase and a 95:5 acetonitrile:water with 0.1% formic acid organic phase. The gradient was as follows: The organic phase composition was 10% for the first 5 min, ramped to 20% for the next 10 min, ramped to 50% for the next 25 min, ramped to 80% in the next 35 min, held at 80% for 10 min followed by a quick ramp to 10% in 5 min, and a 10 min hold to equilibrate the column.

Mass spectrometry was performed on a Thermo Scientific LTQ-FT™, a hybrid instrument consisting of a linear ion trap and an FT-ICR mass spectrometer. The experiments used the standard electrospray source operating with a source voltage of 5 keV and a capillary temperature of 275 °C. Sheath and auxiliary gas flows were 18 and 5 respectively (both Thermo Scientific instrument settings). A typical scan sequence involved a positive ion FT-ICR scan at 100 K resolution (100 K at m/z 400). During the FT-ICR acquisition, six MS/MS scans were acquired by the linear ion trap determining the parent ions from the six most abundant ions observed from a preview of the FT-ICR scan. The CID scans were acquired with an isolation width of 2 and a normalized collision energy of 35 (both Thermo Scientific instrument settings). After acquiring the tandem mass spectra twice, the ion was placed into an exclusion list for 30 s. Charge state screening was enabled with monoisotopic precursor selection.

In this study, two biological replicate experiments were performed. Identification and analysis of peptides containing oxidative modifications were performed using the MassMatrix Program ver. 1.3.1 (32, 33). The modification files were adjusted to include all of the possible oxidative modifications described in references (17, 34). A FASTA library containing all of the spinach PS II subunit protein sequences was searched. Additionally, a decoy library that contained these same proteins but with reversed amino acid sequences was examined. No hits to the decoy library were observed. For the determination of the quality of the peptide calls within MassMatrix, $\max(pp_1, pp_2)$ was ≥ 8.5 and $pp_{Tag} \geq 5.0$ (32, 33). These parameters yield a p value of ≤ 0.00001; only oxidized peptides which exhibited this extremely low p value were considered for the identification of peptides containing oxidized residues. The quality of the mass spectra observed at this high stringency is illustrated in Fig. 1 of references (30) and (35). In this context it should be noted that in MASCOT (software from Matrix Sciences) searches (36), peptide identifications are typically performed with p values ≤ 0.05. The direct consequence of our using such low p values is

that in all cases high quality mass spectra were observed with nearly complete y- and b-ion series for the oxidatively modified peptides. Given the high quality of the data used in this study, the union of the replicate data sets was examined. The identified oxidatively modified residues were mapped onto the *Thermosynechococcus vulcanus* PS II structure (15) of the D1, D2, CP43, and CP47 proteins using PYMOL (37).

RESULTS

As we have reported previously, even in the absence of synchrotron radiation a number of amino acid residues are found to be oxidatively modified in PS II (30, 35). In these earlier studies, seventy-three oxidatively modified amino acid residues were identified in the D1, D2, CP43, and CP47 proteins of spinach PS II at time 0, representing ≈4% of the residues found in these four subunits. That residues are observed to be natively oxidatively modified is not surprising, since the presence of reactive oxygen species (ROS) in the cellular environment and the production of ROS by PS II itself can lead to the oxidative modification of amino acid residues within the photosystem (38–40). Several of these residues are associated with CP43 (^{354}E, ^{355}T, ^{356}M, and $-^{357}$R) and are buried and in close vicinity to the Mn_4CaO_5 cluster. We hypothesized that these residues are associated with an oxygen/ROS exit pathway from the photosystem (30). Additionally, we have reported that subsets of these residues that are associated with the stromal domains of the D1 and D2 proteins are in close proximity to Q_A (D1 residues ^{237}P, ^{238}T, ^{239}F, ^{241}Q, ^{242}E, and the D2 residues ^{237}P, ^{238}T, ^{241}N, and ^{246}M) and $Pheo_{D1}$ (D1 residues ^{130}Q, ^{133}L, and ^{135}Y). The oxidative modification of these residues appears to indicate that both Q_A^- and $Pheo_{D1}^-$ may generate ROS on the reducing side of the photosystem (35).

The oxidative modifications which were observed at the various time points are summarized in supplemental Tables S1-S4, along with the type of oxidative modifications observed and the residue location (surface, buried but in contact with cavity/channel, or buried and not in contact with an apparent cavity/channel) when mapped onto the *T. vulcanus* crystal structure. As noted previously (30), at time 0, the overall sequence coverage observed in this study for the examined proteins was: D1, 24%, D2, 27%, CP47, 41%, and CP43, 26%; the coverage of the residues located in the lumenally exposed extrinsic loops of these proteins, the domains of principal interest in this study, was significantly higher: D1, 35%, D2, 43%, CP47, 55% and CP43, 43%. With increasing irradiation, the sequence coverage improved, such that at 16 s irradiation the overall sequence coverage was: D1, 30%, D2, 33%, CP47, 44%, and CP43, 40% while the coverage of the residues located in the extrinsic loops of these proteins was uniformly higher: D1, 45%, D2, 51%, CP47, 60%, and CP43, 52%. This was expected since oxidative modifications yield peptides which are more hydrophilic and, consequently, more easily resolved by reversed phase chromatography. It should also be noted that not all residues observed to be modified at a particular time point are necessarily observed at all subsequent time points. For instance, 16% of the residues observed to be oxidatively modified in the proteins at 0 s irradiation are not observed at one or more subsequent time points using our stringent peptide selection criteria (*i.e.* $p \leq 10^{-5}$). This is due primarily to the different populations of peptides being present in the irradiated samples (see above) and that only the most abundant peptides, at any particular elution time in the reversed-phase chromatogram, are selected for fragmentation during mass spectrometry. If one lowers the selection criteria to levels typically used in MASCOT searches (*i.e.* $p \leq 0.05$), significantly higher proportions of the peptides are observed at other time points. Using this relaxed criteria, only 9% of the peptides initially identified at high stringency were not observed using the lower stringency criteria. It should also be noted that in no instances were hits to the decoy library observed for any of the examined proteins. In this communication, if a residue was observed to be oxidatively modified at a particular time point, it is assumed to also be modified at subsequent time points with respect to mapping onto the *T. vulcanus* crystal structure.

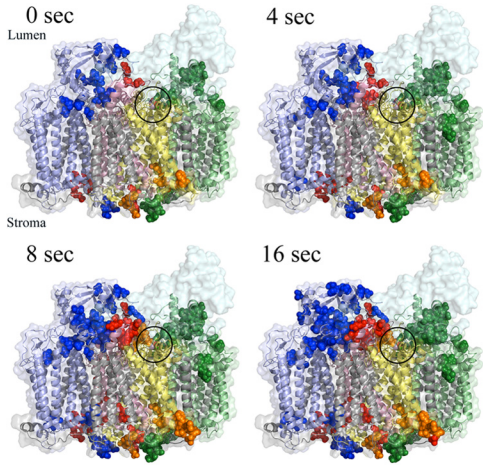

FIGURE 1. **Overview of the time course of oxidatively modified residues identified in the D1, D2, CP43, and CP47 proteins.** Oxidized residues modified after 0, 4, 8, and 16 s of irradiation are shown as spheres mapped onto Monomer I of the *T. vulcanus* structure. Since the PsbU and PsbV subunits are not present in higher plant PS II, these chains are not shown. The view is from outside Monomer I, looking toward the dimeric complex within the plane of the membrane. The lumenal and stromal sides of the membrane are indicated at the 0 s time point. Color key: CP47, *pale blue*; CP43, *pale green*; D1, *pale yellow*; D2, *pale red*; PsbO, *pale cyan*; all other chains, *gray*. The modified residues are shown as *spheres* in darker shades of these colors. The Mn_4O_5Ca cluster is *circled*, and the manganese, oxygen, and calcium are shown as *purple*, *red*, and *bright green spheres*, respectively. Figs. 1–4 were produced using PYMOL (37).

In Figs. 1-4, the accumulation of oxidized residues is presented at the various times shown. Since the D1, D2, CP47, and CP43 proteins are highly homologous between higher plants and cyanobacteria (>85% similarity), it is possible to positionally map the modified residues present on these intrinsic proteins from spinach directly to the corresponding residues in the *T. vulcanus* crystal structure. Of the residues which we observed to be oxidatively modified in spinach, 88% were conserved or conservatively replaced in *T. vulcanus.*

Fig. 1 presents an overview of the time course for the oxidative modification of proteins in the core of PS II. As expected, at all time points the vast majority (≈75%) of the observed modifications were located on the surface of the PS II complex which is exposed to the bulk aqueous solvent. It should be noted that oxidized residues identified at the N terminus of the D1 (^{2}T, ^{3}A ^{4}I, ^{5}L, ^{6}E, ^{7}R, ^{8}R, ^{9}E, and ^{10}S), D2 (^{3}I, ^{7}K, and ^{10}T) and CP43 (^{3}T,

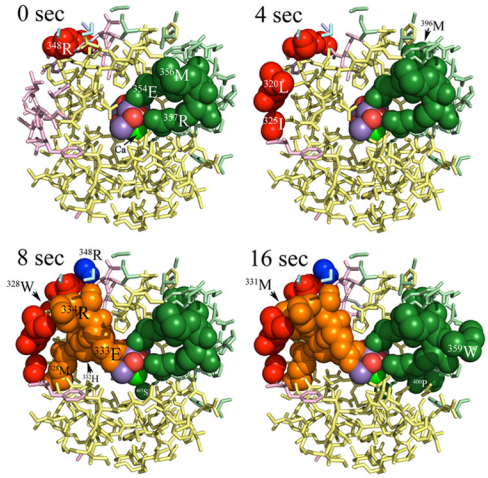

FIGURE 2. **Time course of oxidatively modified residues in the vicinity of the Mn_4O_5Ca cluster active site of PS II.** A 15 Å sphere centered on Mn3 of the Mn_4O_5Ca cluster is illustrated. The orientation is identical to that shown in Fig. 1. Oxidized residues modified after 0, 4, 8, and 16 s of irradiation are shown as *spheres*. Color key: CP47, *pale blue*; CP43, *pale green*; D1, *pale yellow*; D2, *pale red*; PsbO, *pale cyan*. The modified residues are shown in darker shades of these colors. *T. vulcanus* numbering is used. The oxidized residues are labeled at the time of their earliest appearance and are not labeled at subsequent time points. Some residues modified at these various time points are not visible, as they are eclipsed by modified foreground residues. Some unmodified foreground residues, principally of the D1 and D2 chains, have been removed for clarity. The Mn_4O_5Ca cluster is shown with the manganese, oxygen, and calcium illustrated as *purple*, *red*, and *bright green spheres*, respectively. To orient the reader, the Ca of the Mn_4O_5Ca cluster is labeled at the 0 s time point.

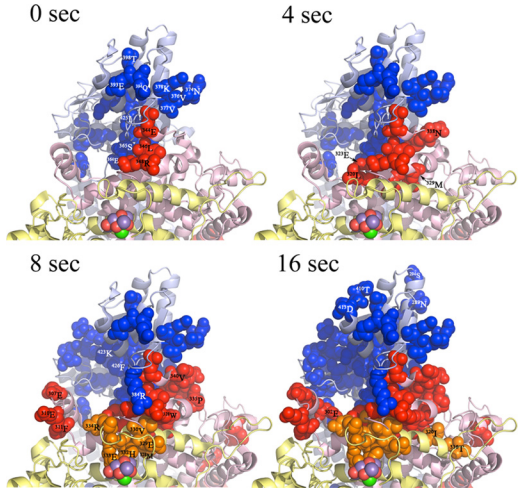

FIGURE 3. **Time course of oxidatively modified residues distant from the Mn_4O_5Ca cluster on the D1, D2 and CP47 proteins.** View is from the Extrinsic Loop E of CP43 looking down onto the Mn_4O_5Ca cluster and residues of the D1, D2, and CP 47 subunits, which are on the lumenal side of the membrane. Oxidized residues modified after 0, 4, 8, and 16 s of irradiation are shown as *spheres*. Color key: CP47, *pale blue*; D1, *pale yellow*; and D2, *pale red*. Only these subunits are illustrated. The modified residues are shown in darker shades of these colors. *T. vulcanus* numbering is used. The oxidized residues are labeled at the time of their earliest appearance and are not labeled at subsequent time points. Some residues modified at these various time points are not visible, as they are eclipsed by other modified foreground residues. The Mn_4O_5Ca cluster is shown with the manganese, oxygen, and calcium illustrated as *purple*, *red*, and *bright green spheres*, respectively.

^{4}L, ^{7}L, and ^{9}R), which were observed at various time points are also probably surface-exposed; however, this could not be verified by direct comparison to the *T. vulcanus* structure, as these residues are not resolved. Consequently, these residues are not included in the calculation above and are not illustrated in Fig. 1. Increasing times of irradiation clearly leads to increased numbers of oxidatively modified residues, most of which are located on the surface of the complex. However, a number of buried residues are also modified. Since these are not in contact with bulk solvent water, the modifying $OH^{\bullet}$ must be produced from buried water molecules located on the interior of the PS II complex. The modified residues appear to form two large groups. The first consists of D1, D2, and CP47 residues, while the second consists of CP43 residues only. Both of these groups of modified residues appear to lead from the Mn_4O_5Ca cluster to modified residues on the surface of the PS II complex.

Fig. 2 illustrates the time course for radiolytic modification of the modified residues which are located within a 15 Å sphere of the Mn_4O_5Ca metal cluster (please note that *T. vulcanus* numbering is used in Figs. 2–5). We had previously reported that at time 0 the residues ^{354}E, ^{355}T, ^{356}M, and ^{357}R of CP43 and residue ^{348}R of the D2 protein are oxidatively modified. This latter residue is exposed on the surface of the complex (30). With increasing irradiation times, additional residues within this sphere become modified. After 4 s irradiation, the D2 residues ^{320}L and ^{325}I as well as CP43:^{396}M of are modified. All of these residues are near the 15 Å boundary and are distant from the M_4O_5Ca cluster. After 8 s irradiation a number of additional residues are observed to be modified; on D1 ^{332}H, ^{333}E, ^{329}E, ^{330}V, ^{334}R, and ^{328}M, D2:^{328}W, CP47:^{384}R, and CP43:^{395}Y and ^{403}S. After 16 s irradiation no modification of additional D2 residues was observed, however, D1:^{331}M and the CP43 residues ^{345}P, ^{359}W, and ^{400}P are oxidatively modified. In Figs. 2–4 some of the residues are not labeled because they are eclipsed by modified residues in the foreground of the figures.

The observed oxidative modifications of the D1 and D2 residues are particularly interesting. For D1, ^{333}E is a bidentate ligand to Mn3 and Mn4 of the metal cluster and ^{332}H is an inner sphere ligand to Mn1. These residues are also in close proximity to $Cl^{-}1$. ^{329}E, ^{334}R, ^{328}M, ^{331}M, and ^{330}V form a distal layer of D1 residues adjacent to ^{333}E and ^{332}H while the D2 residues ^{320}L, ^{321}L, ^{325}I, ^{348}R, and ^{328}W form an additional layer of residues adjacent to the distal D1 residues and more distant from the metal cluster. These latter two residues are surface-exposed. It should also be noted that D2:^{348}R and the adjacent residue, CP47:^{384}R, are also surface-exposed residues.

Fig. 3 illustrates the oxidative modification of residues more distant from the Mn_4O_5Ca cluster. At 4 s the D2 residues ^{329}M, ^{323}E, ^{337}E, ^{338}N, and ^{339}F, are modified. At 8 s the D2 residues ^{307}E, ^{310}E, ^{311}F, ^{335}P, ^{340}V, ^{326}R, ^{327}A, ^{328}W, and ^{336}H, the D1 residues ^{307}E, ^{310}E, and ^{311}F, and the CP47 residues ^{384}R, ^{423}K, and ^{426}F are oxidatively modified. At 16 s D2:^{334}Q and the D1 residues ^{320}I and ^{316}T are modified. At each of these time points additional surface-exposed residues are modified on the D1, D2, and CP47 proteins. The D1, D2, and CP47 residues illustrated in Figs. 2 and 3 form near continuous paths of oxidatively modified residues leading from the surface of the complex to the Mn_4O_5Ca cluster.

Fig. 4 illustrates oxidative modifications of CP43 which are more distant from the Mn_4O_5Ca cluster. At 4 s the surface residues ^{214}L, ^{365}W, ^{393}A, ^{394}E, and ^{396}M are oxidatively modi-

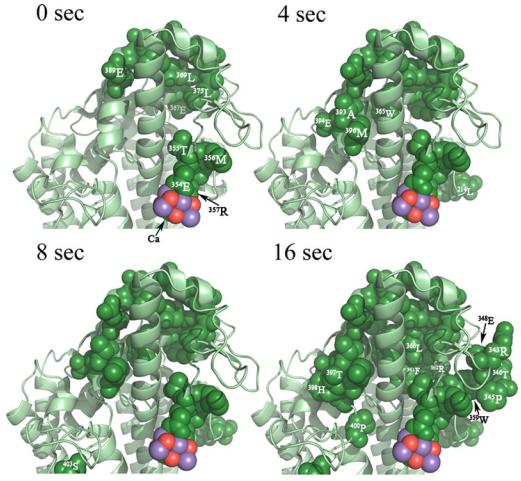

FIGURE 4. **Time course of oxidatively modified residues distant from the Mn_4O_5Ca Cluster on CP43.** View is from the Extrinsic Loop E of CP47 looking down onto the Mn_4O_5Ca cluster and CP43 residues on the lumenal side of the membrane. Oxidized residues modified after 0, 4, 8, and 16 s of irradiation are shown as *spheres*. CP43 is shown in *pale green*. The modified residues are shown as spheres in *darker green*. The oxidized residues are labeled at the time of their earliest appearance and are not labeled at subsequent time points. Some residues modified at these various time points are not visible, as they are eclipsed by modified foreground residues. The Mn_4O_5Ca cluster is shown with the manganese, oxygen, and calcium illustrated as *purple*, *red*, and *bright green spheres*, respectively. To orient the reader, the Ca of the Mn_4O_5Ca cluster is labeled at the 0 s time point.

fied. At 8 s ^{395}Y and ^{403}S are modified. Finally, at 16 s ^{343}R, ^{345}P, ^{346}T, ^{348}E, ^{359}W, ^{361}F, ^{362}R, ^{363}G ^{366}L, ^{397}T, ^{398}H, and ^{400}P exhibit oxidative modifications. At each of these time points additional surface-exposed CP43 residues also exhibit oxidative modifications (a few examples being ^{367}E, ^{368}P, ^{369}L, ^{375}L, ^{376}D, ^{383}D, etc.). Interestingly, in large measure, no prior studies have implicated CP43 being involved in the transit of water from the bulk solvent to the Mn_4O_5Ca cluster, at least in the domains in which we have observed oxidatively modified residues.

DISCUSSION

In this communication we have used the synchrotron radiolysis of water in an attempt to experimentally identify putative water pathways within PS II. Several points must be kept in mind. First, a limitation of our study is that we do not have full mass coverage of all of the domains of the examined proteins exposed to the lumenal side of the membrane. This is, in large measure, a consequence of poor chromatographic resolution of highly hydrophobic peptides. Consequently, our catalogue of oxidatively modified residues is almost undoubtedly incomplete. Additionally, we have examined only the core subunits of PS II -D1, D2, CP43, and CP47. It is probable that residues of other proteins within the complex may participate in the formation of water channels (22, 24, 26, 41). It should also be cautioned that the lack of observed modification of an amino acid residue in no way suggests that the residue is not in contact with water. Finally, photoreduction of the manganese cluster by X-rays could lead to conformational rearrangements within the metal cluster and/or ligating amino acid environment, leading to greater exposure of residues to water and possibly their oxidative modification.

With these caveats in mind, we observe two major groups of oxidized amino acid residues. The first group contains modified amino acid residues identified on D1, D2, and CP47 (Fig. 3). This group extends from D1 residues directly associated as first sphere ligands of the Mn_4O_5Ca cluster (^{332}H and ^{333}E) and other nearby residues on D1 (^{329}E, ^{334}R, ^{328}M, ^{331}M, and ^{330}V) and D2 (^{320}L and ^{348}R). At this point the path bifurcates with one path leading from D2:^{320}L (D2:^{323}E, ^{326}R, and CP47:^{364}S, ^{365}S, ^{363}F, ^{366}F, ^{359}M ^{425}I, and ^{426}F) to CP47:^{423}K, which is exposed at the surface of the complex. Many of the residues in this path are buried and in in contact with cavities and/or channels evident in the *T. vulcanus* crystal structure (see below). A second apparent path leads from D2:^{348}R to the surface residues D2: ^{344}E and ^{346}L and CP47:^{384}R.

The second group of observed oxidized residues consists only of CP43 residues (Fig. 4) and leads from the inner sphere ligand ^{354}E and second sphere ligand ^{357}R to the buried residues ^{355}T and ^{356}M and the surface-exposed ^{359}W. At this point the group bifurcates and one branch of residues (^{345}P, ^{346}T, ^{343}R, and ^{348}E) is in direct contact with the PsbO subunit. While this branch does not appear to reach the lumenal surface, it is possible that PsbO residues complete a putative pathway to the lumen. The second branch of this CP43 pathway includes the buried residues ^{361}F, ^{366}L, and ^{363}G. These residues are in contact with numerous surface-exposed CP43 residues including ^{362}R, ^{367}E, ^{370}R, ^{369}L, ^{375}L, ^{368}P, ^{365}W, etc. Interestingly, no residues in these regions of CP43 have been implicated in any of the proposed models for channels within the photosystem. Many of these residues, however, are in contact with non-contiguous cavities which are present in CP43 and at the CP43: PsbO interface. It is possible that these residues constitute an additional novel water pathway within the PS II complex. Another possibility exists, however. As noted previously (30), the CP43 residues ^{354}E, ^{357}R, ^{355}T, and ^{356}M may be associated with a putative dioxygen/ROS exit pathway. Intriguingly, many of the oxidatively modified CP43 residues identified in this communication extend directly from these four residues, which are in close proximity to the Mn_4O_5Ca cluster, to the lumenal surface of PS II. It is possible that these modified residues form distal portions of a putative dioxygen/ROS egress pathway that is occupied by transient water molecules which could undergo radiolysis. In a variety of other systems the occupation of oxygen channels with water molecules has been documented (42–44). Additionally, any dioxygen remaining in a putative oxygen egress pathway would also be subject to modification during radiolysis, yielding reactive oxygen species (principally $HO_2^{\bullet}$ and $O_2^{\bullet-}$) capable of oxidatively modifying amino acid residues (45). These species can produce oxidative modification of amino acid residues which are indistinguishable from those produced by $OH^{\bullet}$. We hypothesize that the observed CP43 pathway may constitute an oxygen egress pathway leading from the Mn_4O_5Ca cluster to the lumenal surface of the PS II complex. As noted above, no continuous channel connects these CP43 residues forming such a putative dioxygen exit pathway. It is possible that conformational changes occurring during S-state cycling could lead to structural alterations completing a continuous pathway from the Mn_4O_5Ca cluster to the surface of the complex (see below).

Our findings are schematically summarized in Fig. 5. Fig. 5*A* illustrates the oxidized residues found in the D1, D2, and CP47

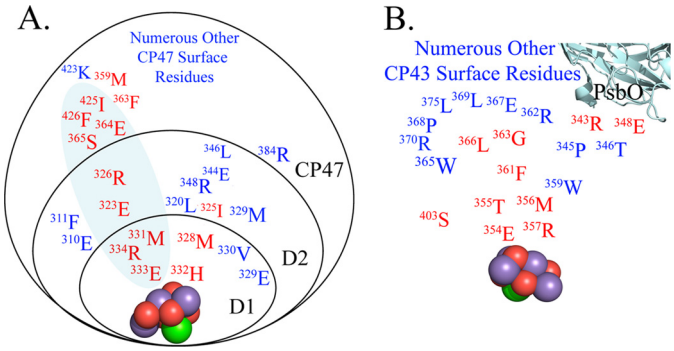

FIGURE 5. **Schematic representation of the groups of modified residues observed in PS II.** *A*, the D1-D2-CP47 group identified as a putative water channel. Each protein is represented as an ellipse. The *cyan* shading indicates the residues associated with the Broad Channel previously identified (26, 41). *B*, the CP43 group hypothesized to be a dioxygen egress pathway or a second water channel. The Mn_4O_5Ca cluster is shown with the manganese, oxygen, and calcium illustrated as *purple*, *red*, and *bright green spheres*, respectively. Buried oxidized residues are shown in *red* while surface-exposed oxidized residues are shown in *blue*.

proteins while Fig. 5*B* shows the modified residues found in CP43. In this figure, the buried residues are highlighted in red while the surface-exposed residues are shown in blue.

Earlier computational studies have identified several putative water/oxygen/proton channels in PS II (22, 24, 41). These studies have been recently reviewed (46). Briefly, 3–5 channels were identified computationally as leading from the lumenal surface of PS II to the Mn_4O_5Ca cluster. Using the nomenclature of Ho (46), these have been termed: 1) the Back Channel, which has been hypothesized to transport either oxygen (22) or water (24, 41), 2) the Narrow Channel, which has been hypothesized to transport protons (24, 41), 3) the Broad Channel, which was hypothesized to transport water and/or protons (22, 24, 41), and 4) the Large Channel, which was hypothesized to transport either water and/or protons (22) or oxygen (24, 41). These studies, in large measure, have utilized computational methodologies (CAVER Analysis and surface contact area analysis). Gabdulkhakov *et al.* (24) additionally performed Xe gas co-crystallization x-ray crystallography. Recently, molecular dynamic simulations coupled with water streamline tracing have been used to map the path of water movement to the oxygen-evolving site (25, 26). These authors identified five putative water channels which, in large measure, are similar to the channels identified in previous studies (see Table 1, Ref. 26). These studies have provided extremely important information concerning the presence of putative channels within the PS II complex and provide a framework for formulating testable hypotheses bearing on the movement of water, oxygen, and protons within the photosystem.

It must be noted, however, that several limitations exist with all of these largely computational studies. These were discussed in detail in our earlier communication (30) with respect to the identification of putative dioxygen/ROS egress pathways. Analogous concerns exist with respect to the identification of putative water pathways. Briefly, since most of the computational studies examine static crystal structures (22, 24, 41), they fail to take into account molecular motion on the nsec time scales which could substantially alter the overall shape and dimensions of the identified water channels within PS II. Vassiliev *et al.* (25, 26) have at least partially addressed this problem using molecular dynamic simulations of water movement within the photosystem. It has also been implicitly assumed that no conformational changes occur in the PS II structure during normal S-state cycling which affect either water transport to the active site (*i.e.* that the overall protein structure observed in the S_1 state is the same as for all of the other S-states) or oxygen away from the active site. S-state transitions, particularly the $S_3 \rightarrow [S_4] \rightarrow S_0$ state transition associated with O_2 formation, release and water binding could affect the location, shape, and dimensions of possible water entrance pathways. A number of studies have indicated that largely undefined conformational changes do occur during S-state cycling (47–50) although the specific residues involved and the effects on putative water channels within the photosystem remain undetermined. It has been noted that even a modest conformational change involving one or a few amino acid residues could hypothetically either open or close a putative water transport (or oxygen transport) channel during S-state cycling (26).

With these caveats in mind, comparison of our results with these computational studies yields some interesting insights. First, as expected, there is no direct one-to-one correspondence between the oxidized residues which we observe and those hypothesized to be in contact with computationally identified putative channels. This is due principally to the lack of complete mass coverage of the examined proteins. Additionally, since we have collected data only on the D1, D2, CP43, and CP47 core subunits of the photosystem, residues on other PS II subunits which contribute to channel formation remain unidentified (22, 24–26, 41). Second, in the protein domains for which we do have mass coverage, comparison to the channels summarized by Ho (Table 1, Ref. 46) yields the following results: in the Back Channel, 22% of the residues were observed to be oxidized, in the Narrow Channel, 33% were modified, and in the Large Channel 35% contained oxidative modifications. Larger numbers of oxidized residues were observed in the Broad Channel, with 55% containing oxidative modifications. Similar results were obtained comparing our data to the channels identified by Vassiliev *et al.* (26). These investigators identified four channels possibly involved in water transit to the Mn_4O_5Ca cluster. A fifth channel, corresponding to the Back Channel of Ho and Styring (41) exhibited a very high energy barrier (22 kcal/mol) for water transport. Of the four putative water channels (designated Channels 1–4 in Ref. 26) which had lower energy barriers (10–15 kcal/mol), residues in contact with Channels 2 and 4 exhibited low amounts of oxidative modification (0 and 22%, respectively). The residues in Channels 1 and 3 which were explicitly identified by the authors exhibited a high degree (67%) of oxidative modification. Consequently, residues located in Channels 1/3, which in large measure corresponds to the Broad Channel of Ho and Styring (41), exhibit a high propensity for oxidative modification in our experiments.

CONCLUSIONS

In this study, we have presented experimental evidence which has identified residues within PS II which are susceptible to modification by $OH^{\bullet}$ produced by synchrotron radiation. We believe that our findings implicate the Broad Channel of Ho and Styring (41) (Channels 1/3 of Vassiliev *et al.* (26)) as a water

channel functioning to deliver substrate water to the Mn_4O_5Ca cluster. A second group consisting entirely of modified CP43 residues was also identified. These residues may be associated with a hypothetical channel which has not been previously been identified. While this putative channel may be a second water channel, we hypothesize that it may constitute a dioxygen/ROS exit pathway leading from the Mn_4O_5Ca cluster to the thylakoid lumen. Experiments are currently ongoing to differentiate between these and other possibilities.

REFERENCES

1. Bricker, T. M., and Burnap, R. L. (2005) in *Photosystem II: The Water/Plastoquinone Oxido-Reductase of Photosynthesis* (Wydrzynski, T., and Satoh, K. eds), pp. 95–120, Springer, Dordrecht
2. Nelson, N., and Yocum, C. F. (2006) Structure and function of Photosystems I and II. *Annu. Rev. Plant Biol.* **57,** 521–565
3. Bricker, T. M., Roose, J. L., Fagerlund, R. D., Frankel, L. K., and Eaton-Rye, J. J. (2012) The extrinsic proteins of Photosystem II. *Biochim. Biophys. Acta* **1817,** 121–142
4. Bricker, T. M., and Frankel, L. K. (1998) The structure and function of the 33 kDa extrinsic protein of Photosystem II. A critical review. *Photosyn. Res.* **56,** 157–173
5. Yi, X., McChargue, M., Laborde, S. M., Frankel, L. K., and Bricker, T. M. (2005) The manganese-stabilizing protein is required for Photosystem II assembly/stability and photoautotrophy in higher plants. *J. Biol. Chem.* **280,** 16170–16174
6. Yi, X., Hargett, S. R., Liu, H., Frankel, L. K., and Bricker, T. M. (2007) The PsbP protein is required for Photosystem II complex assembly/stability and photoautotrophy in Arabidopsis thaliana. *J. Biol. Chem.* **282,** 24833–24841
7. Yi, X., Hargett, S. R., Frankel, L. K., and Bricker, T. M. (2009) The PsbP protein, but not the PsbQ protein, is required for normal thylakoid membrane architecture in *Arabidopsis thaliana*. *FEBS Lett.* **583,** 2142–2147
8. Bricker, T. M., and Frankel, L. K. (2011) Auxiliary functions of the PsbO, PsbP and PsbQ proteins of higher plant Photosystem II: A critical analysis. *J. Photochem. Photobiol.* **104,** 165–178
9. Yi, X., Hargett, S. R., Frankel, L. K., and Bricker, T. M. (2006) The PsbQ protein is required in *Arabidopsis* for Photosystem II assembly/stability and photoautotrophy under low light conditions. *J. Biol. Chem.* **281,** 26260–26267
10. Zouni, A., Witt, H.-T., Kern, J., Fromme, P., Krauss, N., Saenger, W., and Orth, P. (2001) Crystal structure of Photosystem II from *Synechococcus elongatus* at 3.8 Å resolution. *Nature* **409,** 739–743
11. Kamiya, N., and Shen, J.-R. (2003) Crystal structure of oxygen-evolving Photosystem II from *Thermosynechococcus vulcanus* at 3.7 Å resolution. *Proc. Natl. Acad. Sci.* **100,** 98–103
12. Ferreira, K. N., Iverson, T. M., Maghlaoui, K., Barber, J., and Iwata, S. (2004) Architecture of the photosynthetic oxygen-evolving center. *Science* **303,** 1831–1838
13. Loll, B., Kern, J., Saenger, W., Zouni, A., and Biesiadka, J. (2006) Towards complete cofactor arrangement in the 3.0 Å resolution structure of Photosystem II. *Nature* **438,** 1040–1044
14. Guskov, A., Kern, J., Gabdulkhakov, A., Broser, M., Zouni, A., and Saenger, W. (2009) Cyanobacterial photosystem II at 2.9 Å resolution and the roles of quinones, lipids, channels, and chloride. *Nat. Struct. Mol. Biol.* **16,** 334–342
15. Umena, Y., Kawakami, K., Shen, J.-R., and Kamiya, N. (2011) Crystal structure of oxygen-evolving Photosystem II at a resolution of 1.9 Å. *Nature* **473,** 55–60
16. Bricker, T. M., and Ghanotakis, D. F. (1996) Introduction to oxygen evolution and the oxygen-evolving complex. in *Oxygenic Photosynthesis: The Light Reactions* (Ort, D. R., and Yocum, C. F. eds), pp. 113–136, Kluwer Academic Publishers, Dordrecht
17. Takamoto, K., and Chance, M. R. (2006) Radiolytic protein footprinting with mass spectrometry to probe the structure of macromolecular complexes. *Annu. Rev. Biophys. Biomol. Struct.* **35,** 251–276
18. Orban, T., Gupta, S., Palczewski, K., and Chance, M. R. (2010) Visualizing water molecules in transmembrane proteins using raidiolytic labeling methods. *Biochemistry* **49,** 827–834
19. Angel, T. E., Gupta, S., Jastrzebska, B., Palczewski, K., and Chance, M. (2009) Structural waters define a functional channel mediating activation of the GPCR, rhodopsin. *Proc. Natl. Acad. Sci.* **106,** 14367–14372
20. Guan, J. Q., Vorobiev, S., Almo, S. C., and Chance, M. R. (2002) Mapping the G-actin binding surface of cofilin using synchrotron radiation. *Biochemistry* **41,** 5765–5775
21. Liu, R., Guan, J. Q., Zak, O., Aisen, P., and Chance, M. (2003) Structural reorganization of the transferrin c-lobe and transferrin receptor upon complex formation:the c-lobe binds to the receptor helical domain. *Biochemistry* **42,** 12447–12454
22. Murray, J. W., and Barber, J. (2007) Structural characteristics of channels and pathways in Photosystem II including the identification of an oxygen channel. *J. Struct. Biol.* **159,** 228–237
23. Petøek, M., Otyepka, M., Banáš, P., Košinová, P., and Koča, J. (2006) CAVER: A new tool to explore routes from protein clefts, pockets and cavities. *BMC Bioinform.* **7,** 315–315
24. Gabdulkhakov, A., Guskov, A., Broser, M., Kern, J., Müh, F., Saenger, W., and Zouni, A. (2009) Probing the accessibility of the Mn_4Ca cluster in Photosystem II; channels calculation, noble gas derivatization, and cocrystallization with DMSO. *Structure* **17,** 1223–1234
25. Vassiliev, S., Comte, P., Mahboob, A., and Bruce, D. (2010) Tracking the flow of water through PS II using molecular dynamics and streamline tracing. *Biochemistry* **49,** 1873–1881
26. Vassiliev, S., Zaraiskaya, T., and Bruce, D. (2012) Exploring the energetics of water permeation in Photosystem II by multiple steered molecular dynamics simulations. *Biochim. Biophys. Acta* **1817,** 1671–1678
27. Berthold, D. A., Babcock, G. T., and Yocum, C. F. (1981) A highly resolved oxygen-evolving Photosystem II preparation from spinach thylakoid membranes. *FEBS Lett.* **134,** 231–234
28. Ghanotakis, D. F., and Babcock, G. T. (1983) Hydroxylamine as an inhibitor between Z and P_{680} in Photosystem II. *FEBS Lett.* **153,** 231–234
29. Rabilloud, T., Vincon, M., and Garin, J. (1995) Micropreparative one- and two-dimensional electrophoresis: Improvement with new photopolymerization systems. *Electrophoresis* **16,** 1414–1422
30. Frankel, L. K., Sallans, L., Limbach, P. A., and Bricker, T. M. (2012) Identification of oxidized amino acid residues in the vicinity of the Mn_4CaO_5 cluster of Photosystem II: Implications for the identification of oxygen channels within the photosystem. *Biochemistry* **51,** 6371–6377
31. Sun, G., and Anderson, V. E. (2004) Prevention of artifactual protein oxidation generated during sodium dodecyl sulfate-gel electrophoresis. *Electrophoresis* **25,** 959–965
32. Xu, H., and Freitas, M. A. (2007) A mass accuracy sensitive probability based scoring algorithm for database searching of tandem mass spectrometry data. *BMC Bioinform.* **8,** 133–137
33. Xu, H., and Freitas, M. A. (2009) MassMatrix: A database search program for rapid characterization of proteins and peptides from tandem mass spectrometry data. *Proteomics* **9,** 1548–1555
34. Renzone, G., Salzano, A. M., Arena, S., D'Ambrosio, C., and Scaloni, A. (2007) Mass spectrometry-based approaches for structural studies on protein complexes at low-resolution. *Curr. Proteom.* **4,** 1–16
35. Frankel, L. K., Sallans, L., Limbach, P. A., and Bricker, T. M. (2013) Oxidized amino acid residues in the vicinity of Q_A and $Pheo_{D1}$ of the Photosystem II reaction center: Putative generation sites of reducing-side reactive oxygen species. *Plos One* **8,** e58042
36. Perkins, D. N., Pappin, D. J. C., Creasy, D. M., and Cottrell, J. S. (1999) Probability-based protein identification by searching sequence database using mass spectrometry data. *Electrophoresis* **20,** 3551–3567
37. The PyMOL Molecular Graphics System, Version 1.4 Schrödinger, LLC.
38. Pospísil, P., Snyrychová, S., and Naus, J. (2007) Dark production of reactive oxygen species in photosystem II membrane particles at elevated temperature: EPR spin-trapping study. *Biochim. Biophys. Acta* **1767,** 854–859
39. Yamashita, A., Nijo, N., Pospísil, P., Morita, N., Takenaka, D., Aminaka, R., and Yamamoto, Y. (2008) Quality control of Photosystem II: reactive oxygen species are responsible for the damage to Photosystem II under moderate heat stress. *J. Biol. Chem.* **283,** 28380–28391
40. Pospísil, P. (2009) Production of reactive oxygen species by Photosystem

II. *Biochim. Biophys. Acta* **1787,** 1151–1160
41. Ho, F. M., and Styring, S. (2008) Access channels and methanol binding site to the $CaMn_4$ cluster in photosystem II based on solvent accessibility simulations, with implications for substrate water access. *Biochim. Biophys. Acta* **1777,** 140–153
42. Lario, P. I., Sampson, N., and Vrielink, A. (2003) Sub-atomic resolution crystal structure of cholesterol oxidase: what atomic resolution crystallography reveals about enzyme mechanism and the role of the FAD cofactor in redox activity. *J. Mol. Biol.* **326,** 1635–1650
43. Sagermann, M., Ohtaki, A., Newton, K., and Doukyu, N. (2010) Structural characterization of the organic solvent-stable cholesterol oxidase from *Chromobacterium* sp. DS-1. *J. Struct. Biol.* **170,** 32–40
44. Kallio, J. P., Rouvinen, J., Kruus, K., and Hakulinen, N. (2011) Probing the dioxygen route in *Melanocarpus albomyces* laccase with pressurized xenon gas. *Biochemistry* **50,** 4396–4398
45. Maleknia, S. D., Brenowitz, M., and Chance, M. R. (1999) Millisecond radiolytic modification of peptides by synchrotron X-rays identified by mass spectrometry. *Anal. Chem.* **71,** 3965–3973
46. Ho, F. M. (2012) Structural and mechanistic investigations of Photosystem II through computational methods. *Biochim. Biophys. Acta* **1817,** 106–120
47. Noguchi, T., and Sugiura, M. (2001) Flash-induced Fourier transform infrared detection of the structural changes during the S-state cycle of the oxygen-evolving complex in photosystem II. *Biochemistry* **40,** 1497–1502
48. Noguchi, T., and Sugiura, M. (2002) Flash-induced FTIR difference spectra of the water oxidizing complex in moderately hydrated photosystem II core films: effect of hydration extent on S-state transitions. *Biochemistry* **41,** 2322–2330
49. Barry, B. A., Cooper, I. B., De Riso, A., Brewer, S. H., Vu, D. M., and Dyer, R. B. (2006) Time-resolved vibrational spectroscopy detects protein-based intermediates in the photosynthetic oxygen-evolving cycle. *Proc. Natl. Acad. Sci.* **103,** 7288–7291
50. Klauss, A., Sikora, T., Süss, B., and Dau, H. (2012) Fast structural changes (200–900 ns) may prepare the photosynthetic manganese complex for oxidation by Tyr-Z. *Biochim. Biophys. Acta* **1817,** 1196–1207